Ca^{2+} controls slow NAD(P)H oscillations in glucose-stimulated mouse pancreatic islets

Dan S. Luciani[1,2], Stanley Misler[3] and Kenneth S. Polonsky[3]

[1] *Department of Cellular and Physiological Sciences, University of British Columbia, Vancouver, Canada*
[2] *Department of Physics, Technical University of Denmark, Lyngby, Denmark*
[3] *Department of Internal Medicine, Washington University School of Medicine, St Louis, MO, USA*

Exposure of pancreatic islets of Langerhans to physiological concentrations of glucose leads to secretion of insulin in an oscillatory pattern. The oscillations in insulin secretion are associated with oscillations in cytosolic Ca^{2+} concentration ($[Ca^{2+}]_c$). Evidence suggests that the oscillations in $[Ca^{2+}]_c$ and secretion are driven by oscillations in metabolism, but it is unclear whether metabolic oscillations are intrinsic to metabolism or require Ca^{2+} feedback. To address this question we explored the interaction of Ca^{2+} concentration and islet metabolism using simultaneous recordings of NAD(P)H autofluorescence and $[Ca^{2+}]_c$, in parallel with measurements of mitochondrial membrane potential ($\Delta\Psi_m$). All three parameters responded to 10 mM glucose with multiphasic dynamics culminating in slow oscillations with a period of ∼5 min. This was observed in ∼90% of islets examined from various mouse strains. NAD(P)H oscillations preceded those of $[Ca^{2+}]_c$, but their upstroke was often accelerated during the increase in $[Ca^{2+}]_c$, and Ca^{2+} influx was a prerequisite for their generation. Prolonged elevations of $[Ca^{2+}]_c$ augmented NAD(P)H autofluorescence of islets in the presence of 3 mM glucose, but often lowered NAD(P)H autofluorescence of islets exposed to 10 mM glucose. Comparable rises in $[Ca^{2+}]_c$ depolarized $\Delta\Psi_m$. The NAD(P)H lowering effect of an elevation of $[Ca^{2+}]_c$ was reversed during inhibition of mitochondrial electron transport. These findings reveal the existence of slow oscillations in NAD(P)H autofluorescence in intact pancreatic islets, and suggest that they are shaped by Ca^{2+} concentration in a dynamic balance between activation of NADH-generating mitochondrial dehydrogenases and a Ca^{2+}-induced decrease in NADH. We propose that a component of the latter reflects mitochondrial depolarization by Ca^{2+}, which reduces respiratory control and consequently accelerates oxidation of NADH.

(Received 11 November 2005; accepted after revision 31 January 2006; first published online 2 February 2006)
Corresponding author D. S. Luciani: Department of Cellular and Physiological Sciences, University of British Columbia, 2350 Health Sciences Mall, Vancouver, BC, Canada V6T 1Z3. Email: dan.luciani@gmail.com

Glucose-induced insulin release from pancreatic islets of Langerhans depends on glucose uptake and metabolism in the β-cells, which elevates the cytosolic ATP/ADP ratio. This induces closure of ATP-sensitive potassium (K_{ATP}) channels in the plasma membrane (Misler *et al.* 1986; Malaisse & Sener, 1987), leading to cellular depolarization, voltage-gated calcium influx and, ultimately, the stimulation of calcium- and ATP-dependent insulin granule mobilization and exocytosis (Ashcroft & Rorsman, 1989; Misler *et al.* 1992*b*).

A hallmark of the normal insulin secretory response to glucose is its oscillatory nature, both *in vivo* (Lang *et al.* 1979; Porksen *et al.* 1995; Song *et al.* 2000) and *in vitro* in the perfused pancreas (Sturis *et al.* 1994) and isolated islets (Longo *et al.* 1991; Gilon *et al.* 1993; Bergsten *et al.* 1994; Westerlund & Bergsten, 2001). There is evidence that glucose-induced oscillations in islets and β-cells are promoted by periodic cycles in K_{ATP} channel activity (Larsson *et al.* 1996), indicating underlying fluctuations in ATP/ADP ratio and hence the involvement of dynamic metabolic events. Reports of metabolic oscillations in β-cells and islets are consistent with this (Longo *et al.* 1991; Jung *et al.* 2000; Ortsater *et al.* 2000; Ainscow & Rutter, 2002); however, the basis of such oscillations is debated. One possibility is that they are a consequence of enzymatic feedback mechanisms inherent to glycolysis (Tornheim, 1997; Juntti-Berggren *et al.* 2003). However, the picture may be more complex, as increases in cytosolic Ca^{2+} concentration ($[Ca^{2+}]_c$) evoked by glucose, or other agonists that elevate $[Ca^{2+}]_c$, are rapidly relayed to the mitochondria of β-cells in primary islets (Ainscow & Rutter, 2001) and insulin

 DOI: 10.1113/jphysiol.2005.101766

secreting cell lines (Rutter *et al.* 1993; Kennedy *et al.* 1996; Nakazaki *et al.* 1998). The resulting rise in the mitochondrial Ca^{2+} concentration ($[Ca^{2+}]_m$) may both augment oxidative phosphorylation, via activation of intramitochondrial dehydrogenases (McCormack *et al.* 1990*a*,*b*; Civelek *et al.* 1996*b*), and dissipate respiratory energy by the electrogenic uptake and futile cycling of Ca^{2+} across the inner mitochondrial membrane (Magnus & Keizer, 1998*a*; Nicholls & Ferguson, 2002). In the context of the present study, it is important to note that the intimate relationship between $[Ca^{2+}]_c$ and $[Ca^{2+}]_m$ in the β-cell also encompasses a close correlation of oscillatory Ca^{2+} dynamics in the two compartments (Nakazaki *et al.* 1998; Ainscow & Rutter, 2001).

An integral part of the metabolic response of the β-cell to glucose is an increase in the reduced form of endogenous pyridine nucleotides (Panten *et al.* 1973; Duchen *et al.* 1993). Accordingly, the non-invasive measurement of NAD(P)H autofluorescence is an often-used indicator of metabolic activity. Despite prior demonstrations of oscillatory metabolism, oscillations of NAD(P)H autofluorescence have remained elusive in intact islets (Panten *et al.* 1973; Gilon & Henquin, 1992; Patterson *et al.* 2000) and have not been uniformly demonstrated in single primary β-cells. Pralong *et al.* (1990) identified such single-cell oscillations, but this finding was not corroborated by others (Duchen *et al.* 1993; Krippeit-Drews *et al.* 2000; Kindmark *et al.* 2001).

In the present work, we demonstrate and characterize glucose-induced NAD(P)H and mitochondrial membrane potential oscillations in intact mouse islets, and establish a key role of Ca^{2+} in sustaining and shaping these oscillations. This is done, in part, by quantifying the temporal concordance of NAD(P)H and $[Ca^{2+}]_c$ dynamics in islets exposed to glucose and agents that rapidly modulate Ca^{2+} influx. In particular, the simultaneous measurement of $[Ca^{2+}]_c$ and NAD(P)H autofluorescence is achieved by using the Ca^{2+}-sensitive dye Fura Red, whose fluorescent properties allow the joint detection of the relatively weak NAD(P)H autofluorescence signal.

Some of these results have previously been reported in abstract form (Luciani *et al.* 2004).

Methods

Islet isolation and culture

Mouse pancreases were removed in accordance with protocols approved by the Animal Studies Committee of Washington University Medical Center. Mice were given an intraperitoneal injection of pentobarbital sodium (5 mg (100 g body weight)$^{-1}$), followed 5 min later by cervical dislocation. After extraction of the pancreas, islets were isolated by collagenase digestion, using a protocol adapted from that of Lacy & Kostianovsky (1967), and subsequently purified either by centrifugal separation on a discontinuous Ficoll gradient, as previously described (Zhou *et al.* 2000), or by means of filtration through a 70 μm cell strainer, essentially as described by Salvalaggio *et al.* (2002). After isolation and purification, islets were cultured in Gibco RPMI 1640 medium containing 10 mM glucose and supplemented with 100 μU ml^{-1} penicillin, 100 μg ml^{-1} streptomycin and 10% fetal calf serum (pH adjusted to 7.4 with NaOH) at 37°C and 5% CO_2. The following day, islets were hand-picked, transferred to glass coverslips in groups of four to eight and allowed to adhere in culture for 48 h before they were used for imaging. The islets were imaged simultaneously, and were sufficiently separate for there to be no physical contact between them on the coverslip. Except where otherwise indicated, islets from 7- to 12-week-old male C57BL/6 mice were studied.

Islet imaging

For all imaging experiments, coverslips were transferred to a chamber (volume, 1 ml) that was mounted on a temperature-controlled stage and held at 35°C (Medical Systems Corp.) on an inverted microscope (Eclipse TE300, Nikon Inc.) equipped with a ×10 S Fluor objective (Nikon Inc.). Islets were perifused continuously at 2.5 ml min^{-1} with Ringer solution containing (mM): NaCl 144, KCl 5.5, $MgCl_2$ 1, $CaCl_2$ 2, Hepes 20 (pH adjusted to 7.35 with NaOH) and glucose as indicated.

Qualitative estimates of variations in islet mitochondrial membrane potential ($\Delta\Psi_m$) were obtained using the indicator Rhodamine 123 (Rh123), whose fluorescence decreases upon mitochondrial hyperpolarization (Zhou *et al.* 2000). For combined measurements of $[Ca^{2+}]_c$ and NAD(P)H autofluorescence, islets were loaded with the cell permeant acetoxymethyl (AM) ester form of the Ca^{2+} indicator Fura Red. The Ca^{2+}-sensitive dye fura-2 AM was used when $[Ca^{2+}]_c$ was imaged alone. Fura-2 and Fura Red were both loaded at a concentration of 5 μM for 30 min, and Rh123 was loaded at a concentration of 2 μg ml^{-1} for 10 min. All dye loading was done in RPMI medium under standard culture conditions (described above). Prior to image acquisition, islets were washed for 30 min by perifusion with Ringer solution containing either 3 or 10 mM glucose, depending on the nature of the experiment (step increase *versus* steady-state measurement).

Excitation wavelengths were controlled by means of suitable excitation filters (Chroma Technology) mounted in a Lambda DG-4 wavelength switcher (Sutter Instrument Company). NAD(P)H autofluorescence was excited at 365 nm (D365/10 × excitation filter), while both Fura Red and Rh123 were excited at 495 nm (D495/10 × excitation filter). Fura-2 was excited ratiometrically at 340 nm and 380 nm, and the changes in $[Ca^{2+}]_c$ expressed as

the ratio of fluorescence emission intensity at 340 nm (F_{340}) and at 380 nm (F_{380}) (F_{340}/F_{380}). NAD(P)H autofluorescence, and fluorescence of Fura Red and Rh123 were filtered using a DAPI/FITC/TxRed polychroic beamsplitter (Chroma Technology, part number 61002bs) and triple-band emission filter (Chroma Technology, part number 61002m), while a D510/80m wide-band emission filter was used for monitoring fura-2 fluorescence. Images were collected by a CoolSNAP HQ Monochrome 12-bit digital camera (Roper Scientific), and both image acquisition and analysis were controlled by Metafluor software (Universal Imaging Corp.). Unless otherwise indicated, sets of images were acquired every 5 s.

Chemicals

Fura Red AM, fura-2 AM and rhodamine 123 were purchased from Molecular Probes (Eugene, OR, USA). All other chemicals were from Sigma (St Louis, MO, USA).

Data analysis and presentation

To facilitate correlation analyses and comparison of temporal variations, we corrected for the slow downward trend due to photobleaching and dye loss. In experiments examining the stimulated response from baseline (step experiments), the trend was projected by an exponential fitted to pre- and post-stimulus recordings of a minimum duration of 10 min. The trend of steady-state recordings was estimated by an exponential best fit to the full time series. Subsequent division of the raw data by the estimated function effectively removed the slow trend in the time series and expressed fluorescence intensity changes relative to the projected baseline/mean fluorescence. As an increase in $[Ca^{2+}]_c$ leads to a decrease in Fura Red fluorescence, and vice versa, we consistently plotted the Fura Red signal on an inverted scale to give a more intuitive representation of changes in $[Ca^{2+}]_c$. For clarity, a smoothed version of the NAD(P)H time series was occasionally superposed on the raw trace. It should be emphasized, however, that all analyses were performed on the raw data. With the exception of correlation analyses, data processing and plotting were done using the program Igor Pro (Wavemetrics, Inc.). As outlined in previous analyses of pulsatile insulin secretion (Sturis *et al.* 1994), we quantified the oscillatory periods and the temporal lag between simultaneously measured periodic profiles using autocorrelation and cross-correlation analyses, respectively. All correlation estimates were performed on detrended steady-state time series using MATLAB (The Mathworks, Inc.). Results are presented as means ± S.E.M. Differences between means were evaluated using Student's unpaired *t* test, and were considered significant at the 0.05 level.

Results

Phasic NAD(P)H responses to step increases in glucose

To delineate the glucose-induced dynamics of endogenous islet NAD(P)H autofluorescence, we first recorded from islets not loaded with any exogenous fluorophores. Glucose was increased as a step from a substimulatory level of 3 mM to various stimulatory concentrations (Fig. 1). As in previous studies (Panten *et al.* 1973; Gilon & Henquin, 1992; Patterson *et al.* 2000; Zhou *et al.* 2000), islets responded to the increase in extracellular glucose with an initial rapid rise, followed by a sustained elevation in NAD(P)H autofluorescence. However, in contrast to previous studies we observed more complex and often multiphasic NAD(P)H dynamics. The multiphasic response, most consistently seen in islets stepped from 3 to 10 mM glucose, included a transient interruption of the initial NAD(P)H rise, followed by a continued increase and gradual development of slow oscillations superimposed on a plateau (Fig. 1*B*; 25 of 28 islets). The responses to 20 mM glucose were more

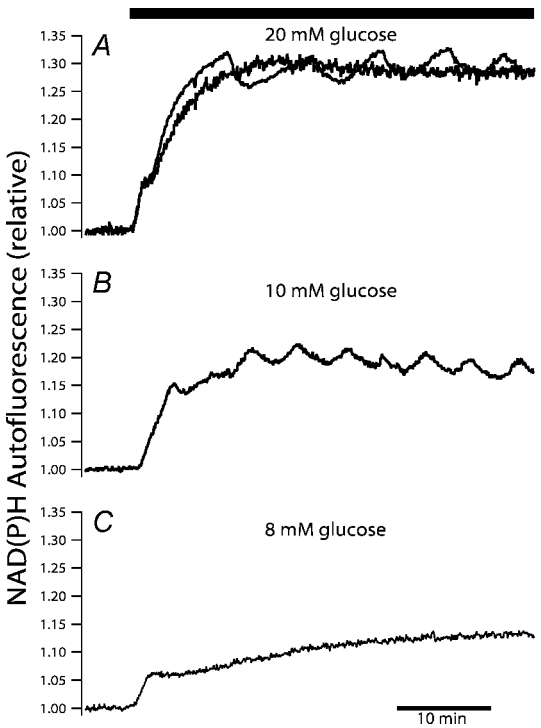

Figure 1. Glucose-induced endogenous islet NAD(P)H autofluorescence changes
Islet NAD(P)H responses to step glucose elevations from a baseline concentration of 3 mM to 20 mM (*A*), 10 mM (*B*) and 8 mM (*C*). Two types of steady-state behaviour were observed upon stimulation with 20 mM glucose (*A*): oscillations and plateau elevations (exemplified by two superimposed traces). The same scale has been used for the three traces to ease comparison. The traces are representative of recordings from 17 (top), 28 (middle) and 15 (bottom) islets. Islets were not loaded with any exogenous fluorescent indicators.

heterogeneous with 9 of 17 islets exhibiting regular oscillations and the remaining eight islets reaching a plateau elevation with no evident oscillations (examples of both shown superimposed in Fig. 1*A*). No discernible oscillations in NAD(P)H autofluorescence were found when the glucose concentration was raised to 8 mM (15 islets in three experiments). As 10 mM glucose most reliably induced oscillations, this concentration was used in our further examination of the dynamics and interactions of islet NAD(P)H and $[Ca^{2+}]_c$.

Correlation of glucose-induced Ca^{2+} and NAD(P)H changes

We next investigated the relationship between glucose-induced changes in islet $[Ca^{2+}]_c$ and NAD(P)H levels by recording simultaneously islet pyridine nucleotide autofluorescence and Fura Red fluorescence. It is well established that a step increase in glucose invokes a triphasic response in $[Ca^{2+}]_c$ consisting of an initial decline (phase 0), followed by a rapid increase to a sustained elevation (phase 1) and finally the development of regular oscillations (phase 2) (Gilon & Henquin, 1992; Bergsten *et al.* 1994; Worley *et al.* 1994). Figure 2*A* shows that islets loaded with Fura Red exhibited this characteristic triphasic $[Ca^{2+}]_c$ response to glucose (Fig. 2*A* lower trace), and that they furthermore exhibit the complex changes in NAD(P)H autofluorescence observed in islets not loaded with the Ca^{2+} indicator (compare Fig. 2*A* upper trace and Fig. 1*B*). In Fig. 2*B* the onset of these responses is shown superimposed and on an expanded timescale. The increase in NAD(P)H fluorescence coincided with that of the phase 0 $[Ca^{2+}]_c$ depression, and preceded the rise in $[Ca^{2+}]_c$ by an average of 2.3 ± 0.2 min ($n = 31$ islets from seven mice). The subsequent NAD(P)H transient, beginning as an acceleration of the initial rise, nearly coincided with the phase 1 $[Ca^{2+}]_c$ peak. However, in a few instances the initial rise in $[Ca^{2+}]_c$ appeared to be associated with a transitory depression of NAD(P)H levels (not shown).

Of 31 islets, in which $[Ca^{2+}]_c$ and NAD(P)H levels were monitored simultaneously, 29 developed oscillations when glucose was increased as a step from 3 to 10 mM. When phase 2 $[Ca^{2+}]_c$ oscillations develop, their period often increases gradually before reaching a steady state. As it also took up to 20 min for the NAD(P)H response to attain a sustained level, we characterized the oscillations, and their temporal correlation, in islets that had been exposed continuously to 10 mM glucose since their isolation 72 h earlier. Unless otherwise indicated, the term 'steady state' refers to recordings under these conditions.

Recordings were also performed on islets from Swiss-Webster and *ob/ob* mice to exclude the possibility that the finding of oscillatory NAD(P)H autofluorescence was specific for islets from the C57BL/6 strain. Islets from these strains responded to a glucose step in a multiphasic manner similar to that of C57BL/6 islets (not shown). Steady-state recordings (Fig. 3*A*) clearly confirmed that the $[Ca^{2+}]_c$ and NAD(P)H dynamics consist of regular, closely associated, oscillations, and furthermore established that this is a phenomenon that generally occurs in mouse islets. We found the temporal and phase characteristics to be maintained throughout the recordings, which were of up to 90 min duration.

The periodicity of the oscillations was determined by autocorrelation analysis of the steady-state time series. Figure 3*B* shows a representative auto-correlogram corresponding to the C57BL/6 recording depicted in Fig. 3*A* (top trace). Significant NAD(P)H autocorrelation coefficients were detected in 33 of 35 islets studied in this manner. The $[Ca^{2+}]_c$ and NAD(P)H oscillations of these islets had a period of 4.7 ± 0.2 min and 4.6 ± 0.2, respectively ($n = 33$ islets from eight mice). These periods

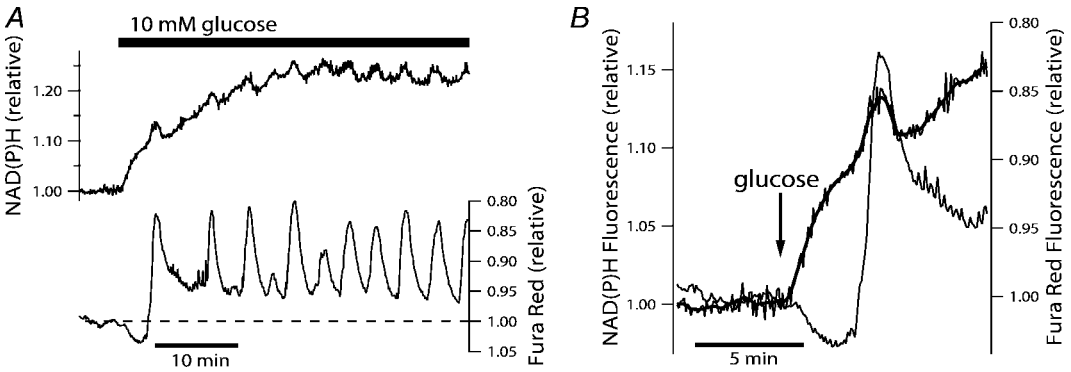

Figure 2. Simultaneous measurement of phasic $[Ca^{2+}]_c$ and NAD(P)H responses
A, long-term dynamics of islet $[Ca^{2+}]_c$ (Fura Red fluorescence) and NAD(P)H autofluorescence changes were measured after a step increase in glucose from 3 to 10 mM. Note the inverted scale on the Fura Red plot, which will be employed in all subsequent Ca^{2+} traces. *B,* expanded and superimposed NAD(P)H and Fura Red responses, illustrating details of the initial phases of the recording shown in *A*.

are plotted in Fig. 3*C*, where the tight clustering around the diagonal (dashed line) confirms that the periods were highly correlated in the individual islets. When not loaded with Fura Red, 49 of 56 islets showed similar steady-state NAD(P)H oscillations (not shown) with a period of 5.1 ± 0.1 min (cf. Fig. 7*B*). We did not perform 'true' steady-state recordings in 20 mM glucose. However, during 40-min segments, starting 20–30 min after a step increase from 3 to 20 mM glucose (cf. Fig. 1), the NAD(P)H oscillations had an average period of 9.3 ± 1.2 min ($n = 9$). This was significantly slower than the steady-state oscillations in 10 mM glucose ($P < 0.01$, for non-loaded islets). It should also be noted that the slight difference in the periods of NAD(P)H oscillations of Fura Red-loaded and non-loaded islets exposed to 10 mM glucose reached statistical significance ($P = 0.02$), hinting at the fact that the Ca^{2+} indicator may not be completely inert at the concentration used.

Though the periods of NAD(P)H and $[Ca^{2+}]_c$ oscillations were nearly identical, a notable feature of the recordings was a phase-shift between the oscillations. We quantified this temporal delay between the $[Ca^{2+}]_c$ and NAD(P)H profiles using cross-correlation analysis. The cross-correlation profile based on the C57BL/6 time series in Fig. 3*A*, is illustrated in Fig. 3*D*. In this example, the peak coefficient is located at a negative lag of five data points corresponding to 25 s. On average, the largest coefficients of Ca^{2+}–NAD(P)H cross-correlation was found at a

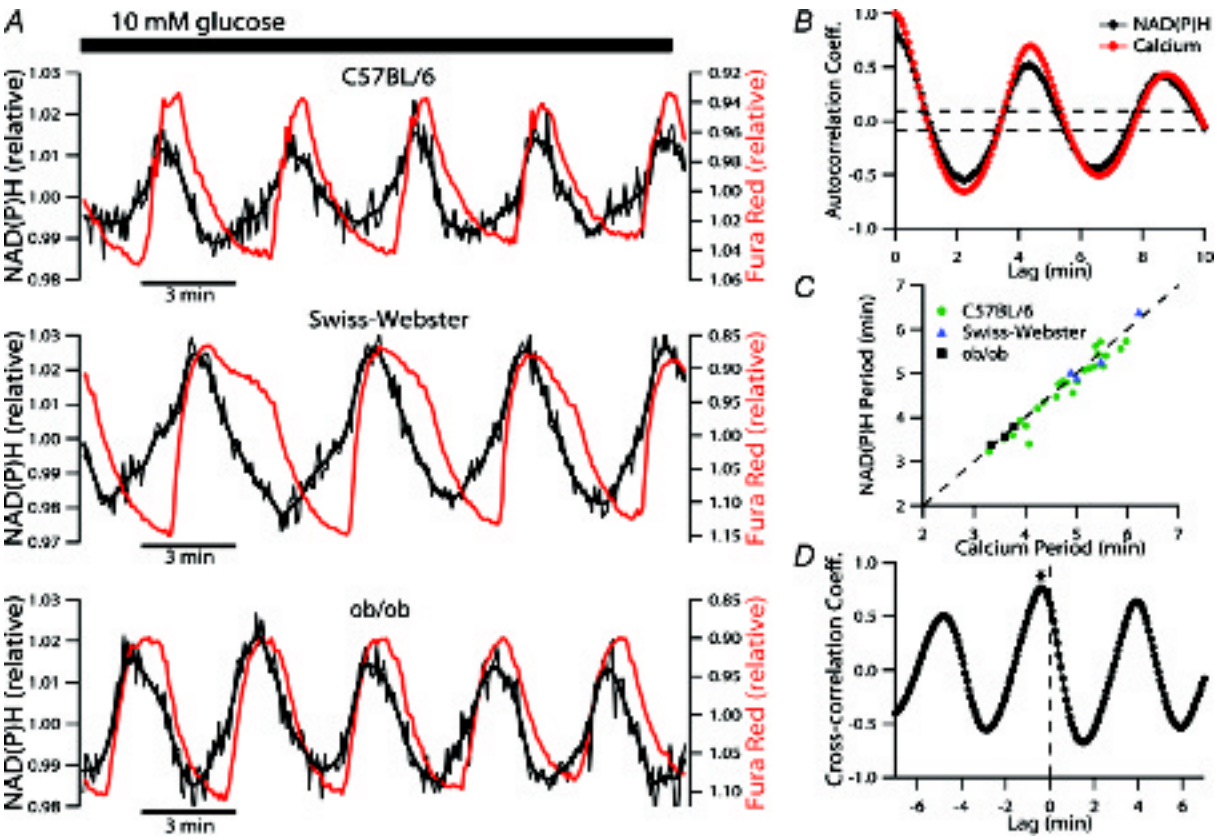

Figure 3. Characterization of steady-state NAD(P)H and $[Ca^{2+}]_c$ oscillations in islets from various strains of mice

A, examples of simultaneously recorded NAD(P)H and $[Ca^{2+}]_c$ oscillations at steady-state in the presence of 10 mM glucose. Islets from three different strains of mice were examined, with the strain indicated above each trace. *B,* sample autocorrelogram quantifying the periodicity of the C57BL/6 islet $[Ca^{2+}]_c$ (red line) and NAD(P)H (black line) oscillations depicted in *A*. The horizontal dashed lines indicate the level of statistical significance of a periodic component and the oscillatory period is determined by the position of the largest positive autocorrelation coefficient to fall outside these boundaries (excluding that at lag zero). *C,* graph of periods of oscillations in $[Ca^{2+}]_c$ *versus* those of the simultaneously measured NAD(P)H oscillations. The data are from 33 islets in which simultaneous steady-state measurements were made for a minimum duration of 40 min. *D,* Ca^{2+}–NAD(P)H cross-correlation coefficients based on the C57BL/6 islet recording shown in *A*. The asterisk indicates the position of the peak coefficient at a negative lag of five data points corresponding to 25 s.

negative lag of 30.6 ± 2.4 s, indicating that NAD(P)H dynamics precede those of $[Ca^{2+}]_c$ by this time (range, 10–70 s, $n = 32$ islets).

Closer inspection of the steady-state profiles revealed that the NAD(P)H upstroke often appeared to be accelerated during the $[Ca^{2+}]_c$ rise. Among the presented examples, this is particularly evident in the islet of the Swiss-Webster mouse (Fig. 3*A* middle trace). This is indicative of metabolic stimulation resulting from an increase in $[Ca^{2+}]_c$, and a direct causal relationship between the two parameters, during the slow islet oscillations.

Ca^{2+} requirement for NAD(P)H oscillations

To investigate possible functions of $[Ca^{2+}]_c$ in shaping the islet NAD(P)H response to glucose, recordings were made under conditions that prevented the normal depolarization-induced Ca^{2+} influx. When the glucose concentration was raised in the presence of the K_{ATP} channel opener diazoxide (Fig. 4*A*), NAD(P)H autofluorescence rose rapidly and reached levels that were not statistically different from those recorded during glucose-induced Ca^{2+} entry ($P = 0.48$, $n = 20$ islets from four mice in both cases). The same observation has previously been made in islets where the glucose concentration was raised under conditions where extracellular Ca^{2+} concentration was kept low by chelation with EGTA (Gilon & Henquin, 1992). In contrast to the multiphasic response we normally observed upon glucose stimulation, the presence of diazoxide resulted in a smooth rise without detectable oscillations. In spite of the hyperpolarization of β-cell membrane potential anticipated under these conditions (Misler *et al.* 1992*a*), there appeared to be a small, gradually developing increase in $[Ca^{2+}]_c$. As this corresponds to a drop in Fura Red fluorescence, it is unlikely to be caused by spillover of NAD(P)H autofluorescence into the Fura Red emission channel, but may rather reflect glucose-augmented efflux of the fluorescent indicator (Arkhammar *et al.* 1989). Upon washout of diazoxide, $[Ca^{2+}]_c$ and NAD(P)H autofluorescence oscillations appeared after a short time (Fig. 4*A*). A crucial role of voltage-gated Ca^{2+} influx in sustaining the slow NAD(P)H oscillations was supported by the finding that the oscillations were reversibly abolished when L-type

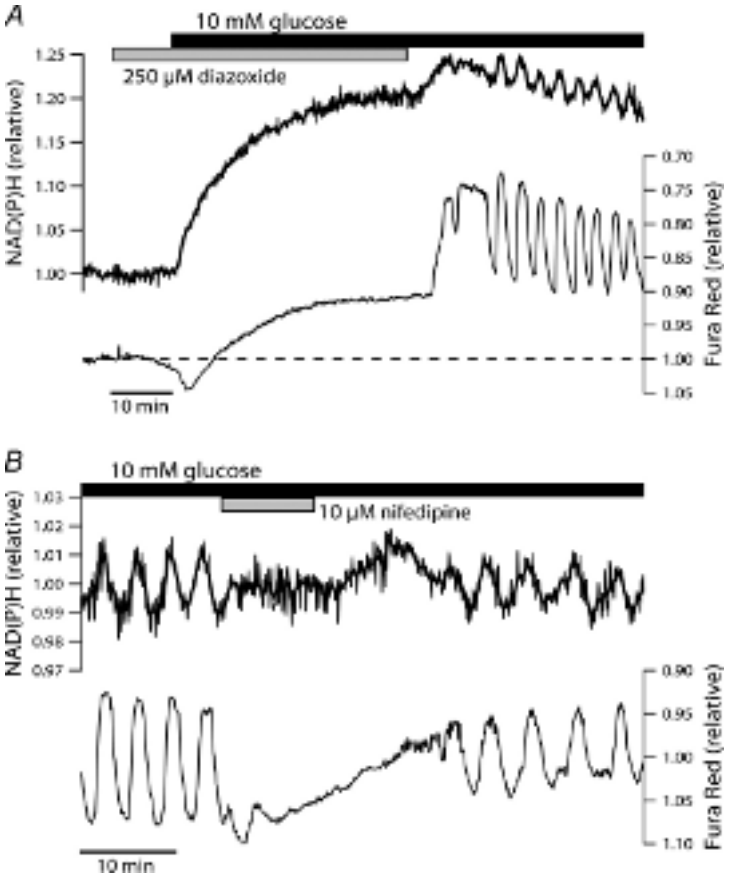

Figure 4. Evidence of Ca^{2+} dependence for the generation of NAD(P)H oscillations
A, the effect of attenuated Ca^{2+} influx on the metabolic response to 10 mM glucose was examined by elevating the glucose concentration in the presence of 250 μM diazoxide (grey bar). Recording is representative of 20 islets from four mice. *B,* blocking L-type voltage-dependent Ca^{2+} channels with 10 μM nifedipine (grey bar) reversibly abolished steady-state NAD(P)H oscillations in the presence of 10 mM glucose. The effect of nifedipine is representative of nine islets from two mice with simultaneously recorded Fura Red fluorescence, and 12 islets from two mice where NAD(P)H autofluorescence was monitored alone (not shown).

Ca^{2+} channels were blocked by the specific inhibitor nifedipine (10 μM) (Fig. 4*B*).

Ca^{2+} exerts dual regulation of islet autofluorescence

The requirement for voltage-dependent Ca^{2+} entry in sustaining NAD(P)H oscillations, together with the apparent Ca^{2+}-induced acceleration of the NAD(P)H upstroke, indicate that slow NAD(P)H oscillations involve stimulation of mitochondrial Ca^{2+}-sensitive dehydrogenases (mCaDH). However, the NAD(P)H downstroke often precedes the fall in $[Ca^{2+}]_c$ during slow islet oscillations. Hence, this stimulatory effect must either be transient, or it must be overcome by another negative effect, which might also be Ca^{2+}-dependent. To examine this possibility, we recorded jointly $[Ca^{2+}]_c$ and NAD(P)H during KCl-induced (30 mM) depolarization of the islet for 10 min, which evoked elevations of $[Ca^{2+}]_c$ lasting longer than the endogenous oscillatory period. When applied to islets equilibrated in 3 mM glucose, KCl induced increases in both $[Ca^{2+}]_c$ and NAD(P)H fluorescence that were maintained for the duration of the depolarization (Fig. 5*A*). Under steady-state conditions in 10 mM glucose, similar sustained depolarization revealed an interesting disparity, namely that the elevation in islet $[Ca^{2+}]_c$ was often paralleled by a reversible drop in NAD(P)H autofluorescence, rather than an increase (Fig. 5*B*). To verify this finding independently of any confounding effects of autonomous fluctuations, the KCl-induced depolarization was repeated in the presence of diazoxide. When islet steady-state electrical activity was suppressed with 100 μM diazoxide, cytosolic $[Ca^{2+}]_c$ fell to the level of the preceding nadir and NAD(P)H oscillations stopped (Fig. 5*C*). Subsequently, the application of a high

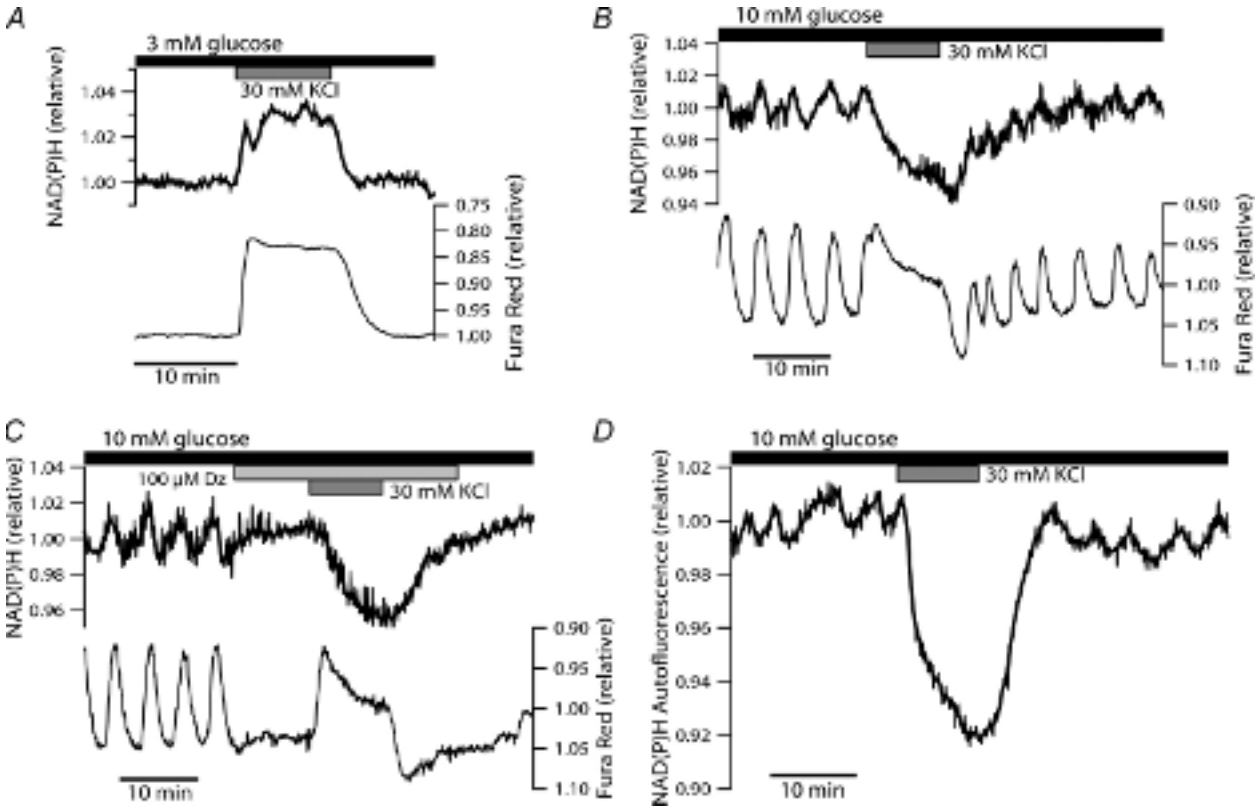

Figure 5. Divergent effects of KCl-evoked Ca^{2+} influx on NAD(P)H autofluorescence in 3 and 10 mM glucose

A, stimulatory effect of depolarization-induced rise in $[Ca^{2+}]_c$ on islet NAD(P)H fluorescence observed in the presence of 3 mM glucose. KCl (30 mM) was applied for 10 min as indicated by the grey bar. The recording is representative of 19 islets from four mice. *B,* effect of 30 mM KCl (grey bar) applied at steady state in the presence of 10 mM glucose. The traces are representative of 10 islets from two experiments. In another experiment with four islets, NAD(P)H oscillations were abolished but NAD(P)H autofluorescence only fell to the level of the oscillatory nadir. *C,* $[Ca^{2+}]_c$ and NAD(P)H response to KCl-induced depolarization in the presence of 100 μM diazoxide (Dz; light grey bar). The recordings are representative of 11 islets in three experiments. *D,* NAD(P)H autofluorescence in response to KCl (30 mM) in islet not loaded with Fura Red. The recording is representative of four islets imaged simultaneously, and five islets from another experiment. The latter showed relative decreases in NAD(P)H autofluorescence comparable in size to those in *B* and *C*.

concentration of KCl raised islet $[Ca^{2+}]_c$ and decreased NAD(P)H autofluorescence, analogous to the observation in the absence of the K_{ATP} channel opener diazoxide. At times, the response was biphasic with an initial transient rise in NAD(P)H fluorescence (not shown). Figure 5*D* illustrates that islets not loaded with Fura Red responded similarly to KCl-induced depolarization. This confirmed that the decrease in NAD(P)H autofluorescence was not due to the presence of the exogenous fluorophore. Thus, increases in $[Ca^{2+}]_c$, comparable in amplitude to the endogenous oscillations, can exert different effects on islet NAD(P)H depending on the prevailing rate of aerobic glucose metabolism.

Role of respiratory chain flux

Using oxygen-sensitive microelectrodes, Kennedy *et al.* (2002; Fig. 6*A* therein) have shown that islets respond with a biphasic, but sustained, increase in oxygen consumption when exposed to KCl in the presence of diazoxide and 10 mM glucose (i.e. a stimulation protocol essentially identical to that employed here in Fig. 5*C*). A decrease in NAD(P)H autofluorescence, concurrent with increased O_2 consumption, conceivably reflects net NADH re-oxidation by NADH dehydrogenase due to acceleration of the electron transport chain. To determine whether the disparate effects of $[Ca^{2+}]_c$ on NAD(P)H levels were associated with the rate of islet respiration, we repeated the KCl protocol during inhibition of electron transfer. Mitochondrial electron transport was inhibited either at complex I by rotenone, or at complex IV using sodium azide (NaN_3), which in the pancreatic β-cell reduces ATP/ADP and causes the cessation of glucose-induced electrical activity by reopening K_{ATP} channels (Misler *et al.* 1992*a*). Respiratory inhibition is known to increase NAD(P)H autofluorescence in a number of cells, including β-cells (Gilon & Henquin, 1992; Krippeit-Drews *et al.* 2000). A large rise in NAD(P)H autofluorescence was also observed here when the inhibitors were applied at steady state in the presence of 10 mM glucose (Fig. 6). This may well be a consequence of diminished NADH oxidation at complex I. It is remarkable that stimulating Ca^{2+} entry with KCl in the presence of either 50 nM rotenone or 3 mM NaN_3 caused a substantial elevation of NAD(P)H autofluorescence on top of the already elevated plateau (Fig. 6). As this additional rise in NAD(P)H autofluorescence most probably reflects augmented tricarboxylic acid cycle flux due to activation of mCaDH, it appears that mitochondrial Ca^{2+} uptake also takes place during inhibition of electron transfer. This is in accord with $[Ca^{2+}]_m$ recordings in INS-1 cells where 20 mM KCl caused a normal increase in $[Ca^{2+}]_m$ in the presence of amytal, a blocker of site I of the respiratory chain (Kennedy & Wollheim, 1998). Taken together these results indicate that, in the glucose-stimulated islet, the net effect of $[Ca^{2+}]_c$ on NAD(P)H autofluorescence is indeed contingent upon the degree of respiratory chain flux, and may represent a balance of mCaDH activation on the one hand, and Ca^{2+}-induced NAD(P)H oxidation on the other.

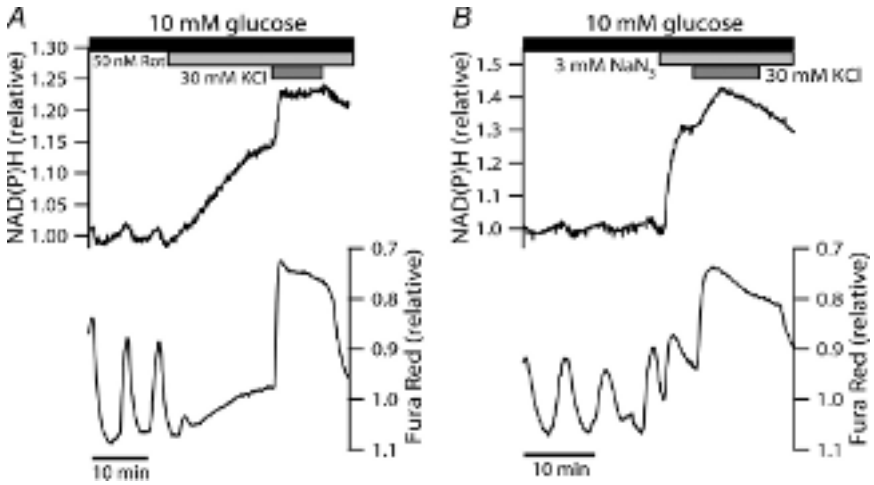

Figure 6. Blockade of islet respiration reverses the NAD(P)H lowering effect of a stimulated $[Ca^{2+}]_c$ rise
Electron transfer in the respiratory chain was blocked during steady-state oscillations in 10 mM glucose by the addition of 50 nM rotenone (Rot; *A*) or 3 mM sodium azide (NaN_3; *B*) (indicated by light grey bars). Both compounds induced a significant rise in NAD(P)H fluorescence which increased further upon depolarization-stimulated Ca^{2+} entry (30 mM KCl; grey bars). Responses are representative of 19 of 20 islets from three mice (rotenone) and 19 islets from four mice (NaN_3). Note that the extended NAD(P)H scale, necessary to view the response to the inhibitors, somewhat obscures the oscillations in the presence of 10 mM glucose.

Ca^{2+}-induced mitochondrial depolarization and $\Delta\Psi_m$ oscillations

It has recently been reported that glucose-induced $[Ca^{2+}]_c$ oscillations induce periodic mitochondrial depolarization in single β-cells and small islet-cell aggregates (Krippeit-Drews *et al.* 2000; Kindmark *et al.* 2001). Because decreasing the $\Delta\Psi_m$ component of the protonmotive force ($\Delta\Psi_m$ and pH difference) will reduce respiratory control, mitochondrial depolarization may accelerate the rate of respiration, and thereby augment NADH oxidation. This prompted us to examine the $\Delta\Psi_m$ dynamics of intact islets, under the same conditions that evoked NAD(P)H and $[Ca^{2+}]_c$ oscillations.

Our measurements demonstrated that islets respond to 10 mM glucose with changes in $\Delta\Psi_m$ that, in their temporal characteristics, closely resemble those of NAD(P)H autofluorescence (Fig. 7). Glucose metabolism rapidly initiated a fall in intensity of Rh123 fluorescence, which reflects the mitochondrial hyperpolarization attributable to matrix proton extrusion, followed by a transient depolarization and concluding with slow oscillations (Fig. 7*A*). This distinctive phasic response was observed in 14 of 16 islets from three mice. Steady-state experiments, at 10 mM glucose, revealed significant $\Delta\Psi_m$ oscillations in 20 of 20 islets (from four mice) with a period of 4.9 ± 0.3 min. This period was not statistically different from that of the NAD(P)H oscillations quantified under similar conditions (Fig. 7*B*).

The experiment in Fig. 7*A* also illustrates the effect of elevated $[Ca^{2+}]_c$ on $\Delta\Psi_m$ in the intact islets. It can be seen that 30 mM KCl evoked a rise in Rh123 fluorescence (i.e. a depolarization of the mitochondria), which persisted for the duration of the stimulation. A comparable lowering of $\Delta\Psi_m$ was observed upon similar exposure to KCl during steady-state oscillations ($n = 11$ islets, not shown). We did not perform joint recordings of $[Ca^{2+}]_c$ and $\Delta\Psi_m$; however, it can be seen in Fig. 7*C* that a stimulation protocol identical to that used in Fig. 7*A* evoked $[Ca^{2+}]_c$ changes that closely mirrored the observed changes in $\Delta\Psi_m$, a good indication that $[Ca^{2+}]_c$ dynamically modulates mitochondrial membrane polarization under

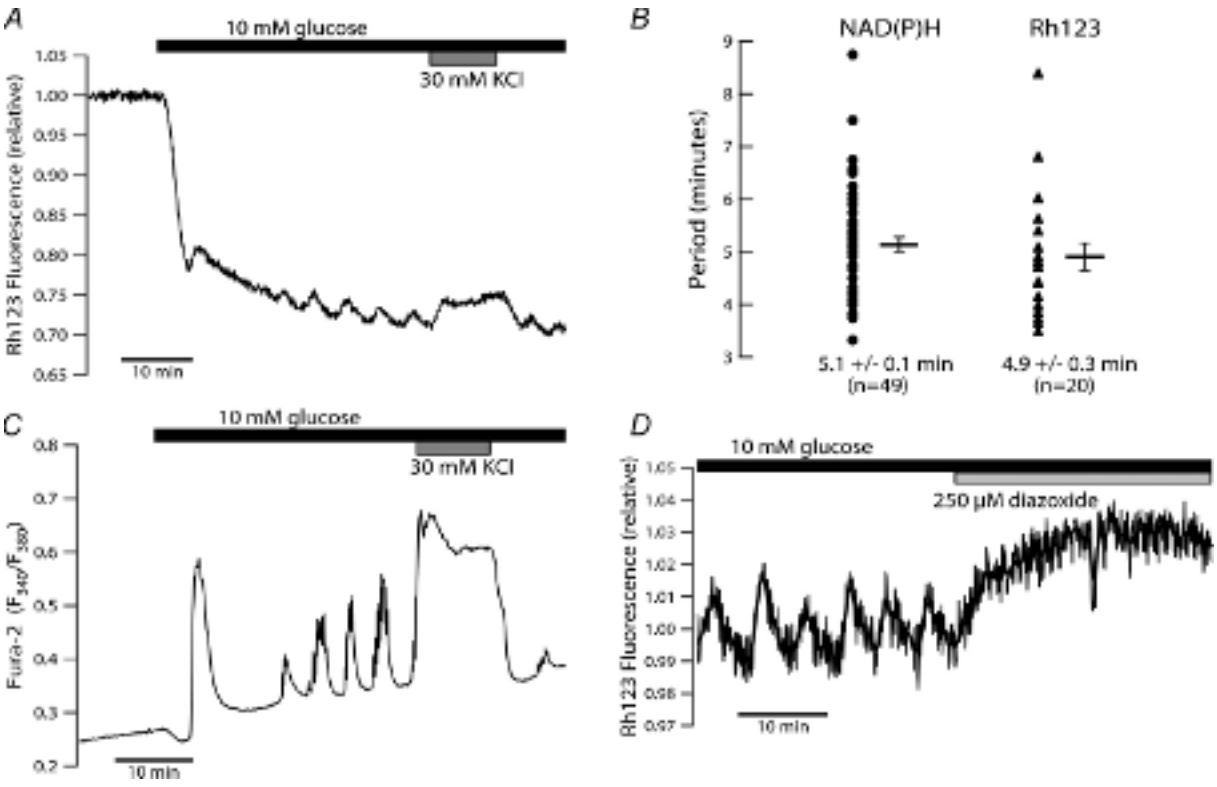

Figure 7. Comparison of changes in islet $\Delta\Psi_m$, $[Ca^{2+}]_c$ and NAD(P)H induced by step increase in glucose
A, the dynamics of islet $\Delta\Psi_m$ in response to a step from 3 to 10 mM glucose were monitored by Rh123 fluorescence. Exposure to 30 mM KCl (grey bar) during slow oscillations evoked a sustained depolarization of $\Delta\Psi_m$. *B,* comparison of the periodicity of NAD(P)H autofluorescence (●) and $\Delta\Psi_m$ (▲) oscillations recorded in islets at steady state in the presence of 10 mM glucose. Measurements were obtained in parallel experiments using islets not loaded with Fura Red. Horizontal bars indicate mean ± S.E.M. *C,* fura-2 recording of islet $[Ca^{2+}]_c$ dynamics evoked by a stimulation protocol analogous to that employed in *A*. *D,* termination of steady-state $\Delta\Psi_m$ oscillations upon islet hyperpolarization by 250 μM diazoxide (light grey bar).

these conditions. When islets were hyperpolarized with diazoxide, the $\Delta\Psi_m$ oscillations disappeared (Fig. 7*D*). Moreover, it was noted that the oscillations were absent during sustained islet depolarization. Thus, clamping islet Ca^{2+} at either high or low levels abolishes oscillations in the mitochondrial membrane potential, which is consistent with the notion that the glucose-induced $\Delta\Psi_m$ oscillations in β-cells derive from a dynamic interrelation with $[Ca^{2+}]_c$ (Magnus & Keizer, 1998*a*; Krippeit-Drews *et al.* 2000; Kindmark *et al.* 2001). When considered in combination, the depolarizing effect of increased $[Ca^{2+}]_c$ on the $\Delta\Psi_m$ and the qualitative and quantitative similarities of $\Delta\Psi_m$ and NAD(P)H dynamics point to the possibility that $[Ca^{2+}]_c$ may also affect NAD(P)H levels by altering respiratory rates via changes in $\Delta\Psi_m$.

Discussion

In the present study we examined the interrelation of glucose-induced $[Ca^{2+}]_c$, NAD(P)H autofluorescence and $\Delta\Psi_m$ responses in intact mouse pancreatic islets. Using the long-wavelength Ca^{2+}-sensitive fluorophore Fura Red, we were able to simultaneously monitor endogenous NAD(P)H autofluorescence and $[Ca^{2+}]_c$ and, thus, to delineate their relationship during the distinct dynamic responses induced by glucose. Parallel measurements of $\Delta\Psi_m$ were made, using average islet Rh123 fluorescence, to further elucidate the interaction of $[Ca^{2+}]_c$ with islet respiration.

Our joint measurements show that the increase in islet NAD(P)H levels precedes the first $[Ca^{2+}]_c$ rise above baseline by approximately 2 min and, hence, that the initiation of β-cell respiration and the subsequent elevation of the ATP/ADP ratio do not require, but rather lead to, the initial rise in $[Ca^{2+}]_c$. This temporal sequence of metabolic and ionic events has previously been observed in studies of glucose-stimulated islets and β-cells, in which $[Ca^{2+}]_c$ and metabolic parameters have been recorded in parallel experiments (Pralong *et al.* 1990; Gilon & Henquin, 1992; Duchen *et al.* 1993; Detimary *et al.* 1998; Patterson *et al.* 2000) or simultaneously (Civelek *et al.* 1996*a*; Jung *et al.* 2000; Krippeit-Drews *et al.* 2000; Kindmark *et al.* 2001). The NAD(P)H response thus coincides with the onset of the characteristic phase 0 drop in $[Ca^{2+}]_c$, which is in agreement with the notion that phase 0 reflects the energy-dependent buffering of basal Ca^{2+} by intracellular organelles via thapsigargin-sensitive uptake (Gylfe, 1988; Chow *et al.* 1995).

Pralong *et al.* (1994) previously reported NAD(P)H fluctuations with a period of approximately 45 s in a subset (~10%) of single isolated rat β-cells. With the exception of these recordings, periodic fluctuations in steady-state NAD(P)H levels have remained elusive in investigations of intact islets (Panten *et al.* 1973; Gilon & Henquin, 1992) and single β-cells (Krippeit-Drews *et al.* 2000; Kindmark *et al.* 2001). Contrary to the former islet studies, our findings demonstrate that intermediate concentrations of glucose reliably induce multiphasic NAD(P)H dynamics culminating in slow and regular oscillations. It remains unclear, however, exactly why we so consistently observed these islet oscillations while they have escaped detection in other studies. As islets from C57BL/6, Swiss-Webster and *ob/ob* mice showed similar behaviour, it is highly unlikely that the difference is directly related to the mouse strain under investigation.

Because of the elusive nature of oscillations of NAD(P)H autofluorescence, there has thus far been no direct information regarding the temporal concordance of oscillatory islet $[Ca^{2+}]_c$ and NAD(P)H dynamics under physiological steady-state conditions. We established that at 10 mM glucose, the NAD(P)H oscillations have a period of roughly 5 min and are highly correlated with, but consistently lead, oscillations in $[Ca^{2+}]_c$, as demonstrated by their joint measurement. Furthermore we found that voltage-gated Ca^{2+} influx is a prerequisite for these slow NAD(P)H oscillations (Fig. 4). This is analogous to a dependence on extracellular Ca^{2+} observed for the faster NAD(P)H fluctuations of single rat β-cells (Pralong *et al.* 1994), an indication that fast and slow NAD(P)H dynamics to some degree share a common basis.

Similar to the situation in a variety of other cell types, mitochondria of β-cells sequester Ca^{2+} in response to increases in $[Ca^{2+}]_c$ induced under physiological conditions (Rutter *et al.* 1993; Kennedy *et al.* 1996; Nakazaki *et al.* 1998; Ainscow & Rutter, 2001). This can affect the cellular energy state via stimulation of intramitochondrial Ca^{2+}-sensitive dehydrogenases (McCormack *et al.* 1990*a*,*b*). Our recordings provide indirect evidence that, during physiological stimulation of pancreatic islets by glucose, $[Ca^{2+}]_c$ dynamically activates these enzymes and increases the rate of TCA cycle flux. This manifests itself already during the initial phase of the response, where a transitory acceleration of the gradual NAD(P)H rise coincided with the peak in $[Ca^{2+}]_c$ (Fig. 2). Previously it has been demonstrated that $[Ca^{2+}]_c$ transients, induced by brief (30 s) pulses of a high concentration of KCl, initiate parallel pulses of NAD(P)H formation in quiescent rat β-cells in the presence of basal levels of glucose (Pralong *et al.* 1994). We found that extended periods of KCl-induced depolarization evokes similar metabolic stimulation of intact islets exposed to 3 mM glucose (Fig. 5*A*), which matches a rise in cytosolic ATP levels observed in rat islets depolarized under similar conditions (Ainscow & Rutter, 2001). While glucose-induced NAD(P)H oscillations could thus arise as $[Ca^{2+}]_c$ oscillations are relayed to the mitochondria and periodically stimulate mCaDH, a number of our observations indicate that slow steady-state NAD(P)H

oscillations are a manifestation of a more complex effect of elevated $[Ca^{2+}]_c$ on the islet redox state. First, rises in NAD(P)H generally precede those of $[Ca^{2+}]_c$ during spontaneous oscillations (Fig. 3). Second, while activation of mCaDH augments oscillations in NAD(P)H autofluorescence, prolonged rises in $[Ca^{2+}]_c$ tend to decrease NAD(P)H levels (Fig. 5). Conceivably this effect comes into play during slow glucose-induced oscillations and contributes to the NAD(P)H autofluorescence downstroke. The lowering of NAD(P)H induced by Ca^{2+} is in contrast to the stimulation observed in presence of basal levels of glucose, and hinges on maintained flux through the electron transport chain (Fig. 6). Two principal mechanisms may account for this observation, namely the inhibition of β-cell phosphofructokinase, and hence glycolysis, by mitochondrially derived ATP (Yaney *et al.* 1995) and/or augmented NADH oxidation independent of changes in TCA cycle activity.

Hepatocytes stimulated by vasopressin show increases in NAD(P)H levels that return to prestimulatory levels despite sustained activation of pyruvate dehydrogenase (Robb-Gaspers *et al.* 1998). This is paralleled by an increase in the protonmotive force, and has therefore been attributed to NAD(P)H re-oxidation evoked by direct, Ca^{2+}-dependent activation of the respiratory chain, possibly involving mitochondrial volume changes (Robb-Gaspers *et al.* 1998). In light of the present results we surmise that rises in islet NAD(P)H autofluorescence due to mCaDH activation are also countered by Ca^{2+}-induced NADH oxidation. However, because islet $\Delta\Psi_m$ is depolarized, rather than hyperpolarized, under conditions that lower NAD(P)H autofluorescence (cf. Figs 5 and 7*A*), the islet NAD(P)H re-oxidation is more likely to be a consequence of reduced respiratory control caused by the fall in the protonmotive force. The lowering of $\Delta\Psi_m$ is presumably due to the continuous futile mitochondrial cycling of Ca^{2+} (Magnus & Keizer, 1998*a*; Krippeit-Drews *et al.* 2000; Kindmark *et al.* 2001). The NAD(P)H and $\Delta\Psi_m$ measurements made here corroborate the presence of slow (> 3 min) oscillations in islet respiration, as previously documented by high resolution O_2 recordings (Longo *et al.* 1991; Jung *et al.* 2000; Ortsater *et al.* 2000). In agreement with our findings, Jung *et al.* (2000) established that the O_2 oscillations depended on Ca^{2+} influx. It is interesting that they also found that an oscillation in $[Ca^{2+}]_c$ precedes that of O_2 consumption. This is reconcilable with the observed oscillatory Ca^{2+}–NAD(P)H phase relationship, as both a rise in NAD(P)H autofluorescence (mCaDH stimulation) and augmented NADH oxidation by the respiratory chain may be associated with increased respiratory flux and, consequently, a lowering of O_2 levels.

Thus, our results suggest that $[Ca^{2+}]_c$ plays an important role in the generation of slow oscillations in islet respiration. Nevertheless, it remains a possibility that Ca^{2+}-independent oscillations exist that are merely too weak to be detected by the measurement techniques employed here. K_{ATP} channel activity in the β-cell has been reported to oscillate with periods between 2.5 and 4 min in the presence of substimulatory glucose levels where voltage-gated Ca^{2+} influx is not activated (Dryselius *et al.* 1994). There is conflicting evidence regarding the role of Ca^{2+} in sustaining O_2 oscillations. In contrast to the findings of Jung *et al.* (2000), other islet studies (Longo *et al.* 1991; Ortsater *et al.* 2000) and measurements from insulin-secreting clonal (HIT) β-cells (Porterfield *et al.* 2000) have identified low-amplitude O_2 oscillations in the presence of basal levels of glucose and under Ca^{2+}-free conditions. The latter were, however, significantly amplified upon elevation of the Ca^{2+} concentration.

The phase relationship observed in our steady-state recordings is consistent with a scenario where metabolic oscillations, via regulation of the K_{ATP} channel, induce slow oscillations of $[Ca^{2+}]_c$ and, ultimately, insulin secretion. Metabolic oscillations in the β-cell have been proposed to arise from intrinsic glycolytic mechanisms involving the allosteric feedback-activation of phosphofructokinase (Tornheim, 1997; Juntti-Berggren *et al.* 2003). That glycolytic flux is oscillatory has been demonstrated by recordings of oscillations in islet glucose consumption (Jung *et al.* 2000) and islet lactate release (Chou *et al.* 1992). However, a purely glycolytic basis of these oscillations is in apparent conflict with the Ca^{2+} requirement for oscillations in NAD(P)H and $\Delta\Psi_m$, which rather supports the presence of a full feedback loop where oscillations in $[Ca^{2+}]_c$ and metabolism arise through a mutual interdependence.

Several mechanisms have been proposed by which $[Ca^{2+}]_c$ feedback may reduce cellular ATP levels and re-activate the K_{ATP} channels (reviewed by Kennedy *et al.* 2002). These include: (i) Ca^{2+}-stimulated ATP hydrolysis (Detimary *et al.* 1998; Ainscow & Rutter, 2002); (ii) reduced ATP synthesis due to futile mitochondrial Ca^{2+} cycling (Magnus & Keizer, 1998*a*; Krippeit-Drews *et al.* 2000; Kindmark *et al.* 2001); and (iii) Ca^{2+}-dependent feedback inhibition of glycolytic flux (Jung *et al.* 2000). Our results are most directly compatible with the second of these possibilities, but do not rule out the other ATP-lowering mechanisms. When considering this, it should also be kept in mind that both futile mitochondrial cycling of Ca^{2+} and increased cytosolic ATP consumption may in fact accelerate respiration by attenuating respiratory control. Consequently, for the Ca^{2+}-dependent negative feedback mechanisms to repolarize the β-cell, it is necessary that the sum of their effects exceed this compensatory increase in oxidative phosphorylation.

Conversely, the putative impact of the recorded NAD(P)H autofluorescence and $\Delta\Psi_m$ oscillations on islet $[Ca^{2+}]_c$ and secretion dynamics depends on their ability to effectively change the rate of oxidative phosphorylation. Based on detailed mathematical modelling of β-cell mitochondrial metabolism and calcium handling it has been predicted that $\Delta\Psi_m$ oscillations with an amplitude of less than 1 mV provide adequate regulation of ATP synthesis to induce K_{ATP} channel-dependent bursting electrical behaviour (Magnus & Keizer, 1998*a*,*b*). In the model, the size of these $\Delta\Psi_m$ fluctuations is approximately 10% of the total mitochondrial hyperpolarization observed upon a simulated glucose rise, and the corresponding mitochondrial NADH oscillations have an amplitude of roughly 20% of the total glucose-induced NADH rise (Magnus & Keizer, 1998*b*). These theoretical estimates are comparable to the experimental observations in the present study. This supports the possibility that the recorded metabolic oscillations are of functional consequence and, hence, that the interactions between Ca^{2+} concentration and respiration are in fact of a reciprocal nature. A more quantitative verification of these model predictions is an important task to be addressed in future experiments.

In addition to the scenarios discussed above, there is a composite model in which an intrinsic slow glycolytic oscillator co-exists with indirect Ca^{2+}-dependent modulation of glycolytic flux. This alternative model has been constructed and examined mathematically (Bertram *et al.* 2004) and extending this work promises to provide further insights into the fundamental, yet remarkably complex, questions of how Ca^{2+}, glycolysis and mitochondria interact to regulate β-cell oscillatory behaviour.

In summary, the present work has established that glucose consistently induces slow NAD(P)H autofluorescence oscillations in intact mouse pancreatic islets, and clarified how these arise through interaction with changes in Ca^{2+} concentration. The data indicate that $[Ca^{2+}]_c$ shapes the NAD(P)H oscillations by first accelerating the reduction of pyridine nucleotides and then invoking the subsequent drop in NAD(P)H autofluorescence, in part by stimulating NADH oxidation in the electron transport chain. When $[Ca^{2+}]_c$ falls at the end of an oscillation, NAD(P)H levels can once again increase to complete the periodic cycle. Moreover, our findings provide evidence to support the hypothesis that slow glucose-induced oscillations in islet respiration depend on feedback interactions between ionic and metabolic events in the pancreatic β-cell. These dynamic cross-talk mechanisms are therefore likely to be essential for normal pulsatile insulin release dynamics and may potentially be compromised when this pulsatility of insulin release is impaired in the development of type 2 diabetes.

References

Ainscow EK & Rutter GA (2001). Mitochondrial priming modifies Ca^{2+} oscillations and insulin secretion in pancreatic islets. *Biochem J* **353**, 175–180.

Ainscow EK & Rutter GA (2002). Glucose-stimulated oscillations in free cytosolic ATP concentration imaged in single islet β-cells: evidence for a Ca^{2+}-dependent mechanism. *Diabetes* **51**, S162–S170.

Arkhammar P, Nilsson T & Berggren PO (1989). Glucose-stimulated efflux of fura-2 in pancreatic beta-cells is prevented by probenecid. *Biochem Biophys Res Commun* **159**, 223–228.

Ashcroft FM & Rorsman P (1989). Electrophysiology of the pancreatic beta-cell. *Prog Biophys Mol Biol* **54**, 87–143.

Bergsten P, Grapengiesser E, Gylfe E, Tengholm A & Hellman B (1994). Synchronous oscillations of cytoplasmic Ca^{2+} and insulin release in glucose-stimulated pancreatic islets. *J Biol Chem* **269**, 8749–8753.

Bertram R, Satin L, Zhang M, Smolen P & Sherman A (2004). Calcium and glycolysis mediate multiple bursting modes in pancreatic islets. *Biophys J* **87**, 3074–3087.

Chou HF, Berman N & Ipp E (1992). Oscillations of lactate released from islets of Langerhans: evidence for oscillatory glycolysis in beta-cells. *Am J Physiol* **262**, E800–E805.

Chow RH, Lund PE, Loser S, Panten U & Gylfe E (1995). Coincidence of early glucose-induced depolarization with lowering of cytoplasmic Ca^{2+} in mouse pancreatic beta-cells. *J Physiol* **485**, 607–617.

Civelek VN, Deeney JT, Kubik K, Schultz V, Tornheim K & Corkey BE (1996*a*). Temporal sequence of metabolic and ionic events in glucose-stimulated clonal pancreatic beta-cells (HIT). *Biochem J* **315**, 1015–1019.

Civelek VN, Deeney JT, Shalosky NJ, Tornheim K, Hansford RG, Prentki M & Corkey BE (1996*b*). Regulation of pancreatic beta-cell mitochondrial metabolism: influence of Ca^{2+}, substrate and ADP. *Biochem J* **318**, 615–621.

Detimary P, Gilon P & Henquin JC (1998). Interplay between cytoplasmic Ca^{2+} and the ATP/ADP ratio: a feedback control mechanism in mouse pancreatic islets. *Biochem J* **333**, 269–274.

Dryselius S, Lund PE, Gylfe E & Hellman B (1994). Variations in ATP-sensitive K^+ channel activity provide evidence for inherent metabolic oscillations in pancreatic beta-cells. *Biochem Biophys Res Commun* **205**, 880–885.

Duchen MR, Smith PA & Ashcroft FM (1993). Substrate-dependent changes in mitochondrial function, intracellular free calcium concentration and membrane channels in pancreatic beta-cells. *Biochem J* **294**, 35–42.

Gilon P & Henquin JC (1992). Influence of membrane potential changes on cytoplasmic Ca^{2+} concentration in an electrically excitable cell, the insulin-secreting pancreatic B-cell. *J Biol Chem* **267**, 20713–20720.

Gilon P, Shepherd R & Henquin J (1993). Oscillations of secretion driven by oscillations of cytoplasmic Ca^{2+} as evidences in single pancreatic islets. *J Biol Chem* **268**, 22265–22268.

Gylfe E (1988). Nutrient secretagogues induce bimodal early changes in cytoplasmic calcium of insulin-releasing ob/ob mouse beta-cells. *J Biol Chem* **263**, 13750–13754.

Jung SK, Kauri LM, Qian WJ & Kennedy RT (2000). Correlated oscillations in glucose consumption, oxygen consumption, and intracellular free Ca^{2+} in single islets of Langerhans. *J Biol Chem* **275**, 6642–6650.

Juntti-Berggren L, Webb DL, Arkhammar PO, Schultz V, Schweda EK, Tornheim K & Berggren PO (2003). Dihydroxyacetone-induced oscillations in cytoplasmic free Ca^{2+} and the ATP/ADP ratio in pancreatic beta-cells at substimulatory glucose. *J Biol Chem* **278**, 40710–40716.

Kennedy ED, Rizzuto R, Theler JM, Pralong WF, Bastianutto C, Pozzan T & Wollheim CB (1996). Glucose-stimulated insulin secretion correlates with changes in mitochondrial and cytosolic Ca^{2+} in aequorin-expressing INS-1 cells. *J Clin Invest* **98**, 2524–2538.

Kennedy ED & Wollheim CB (1998). Role of mitochondrial calcium in metabolism-secretion coupling in nutrient-stimulated insulin release. *Diabetes Metab* **24**, 15–24.

Kennedy RT, Kauri LM, Dahlgren GM & Jung S-K (2002). Metabolic oscillations in β-cells. *Diabetes* **51**, S152–S161.

Kindmark H, Kohler M, Brown G, Branstrom R, Larsson O & Berggren P-O (2001). Glucose-induced oscillations in cytoplasmic free Ca^{2+} concentration precede oscillations in mitochondrial membrane potential in the pancreatic beta-cell. *J Biol Chem* **276**, 34530–34536.

Krippeit-Drews P, Dufer M & Drews G (2000). Parallel oscillations of intracellular calcium activity and mitochondrial membrane potential in mouse pancreatic B-cells. *Biochem Biophys Res Commun* **267**, 179–183.

Lacy PE & Kostianovsky M (1967). Method for the isolation of intact islets of Langerhans from the rat pancreas. *Diabetes* **16**, 35–39.

Lang DA, Matthews DR, Peto J & Turner RC (1979). Cyclic oscillations of basal plasma glucose and insulin concentrations in human beings. *N Engl J Med* **301**, 1023–1027.

Larsson O, Kindmark H, Branstrom R, Fredholm B & Berggren P-O (1996). Oscillations in K_{ATP} channel activity promote oscillations in cytoplasmic free Ca^{2+} concentration in the pancreatic β cell. *Proc Natl Acad Sci U S A* **93**, 5161–5165.

Longo E, Tornheim K, Deeney J, Varnum B, Tillotson D, Prentki M & Corkey B (1991). Oscillations in cytosolic free Ca^{2+}, oxygen consumption, and insulin secretion in glucose-stimulated rat pancreatic islets. *J Biol Chem* **266**, 9314–9319.

Luciani DS, Misler S & Polonsky KS (2004). Temporal concordance of glucose-induced NAD(P)H and Ca^{2+} oscillations measured simultaneously in mouse pancreatic islets. *Biophys J* **86**(Suppl 1), 470a.

Magnus G & Keizer J (1998*a*). Model of beta-cell mitochondrial calcium handling and electrical activity. I. Cytoplasmic variables. *Am J Physiol* **274**, C1158–C1173.

Magnus G & Keizer J (1998*b*). Model of beta-cell mitochondrial calcium handling and electrical activity. II. Mitochondrial variables. *Am J Physiol* **274**, C1174–C1184.

McCormack JG, Halestrap AP & Denton RM (1990*a*). Role of calcium ions in regulation of mammalian intramitochondrial metabolism. *Physiol Rev* **70**, 391–425.

McCormack JG, Longo EA & Corkey BE (1990*b*). Glucose-induced activation of pyruvate dehydrogenase in isolated rat pancreatic islets. *Biochem J* **267**, 527–530.

Malaisse WJ & Sener A (1987). Glucose-induced changes in cytosolic ATP content in pancreatic islets. *Biochim Biophys Acta* **927**, 190–195.

Misler S, Barnett DW & Falke LC (1992*a*). Effects of metabolic inhibition by sodium azide on stimulus-secretion coupling in B cells of human islets of Langerhans. *Pflugers Arch* **421**, 289–291.

Misler S, Barnett DW, Gillis KD & Pressel DM (1992*b*). Electrophysiology of stimulus-secretion coupling in human beta-cells. *Diabetes* **41**, 1221–1228.

Misler S, Falke LC, Gillis K & McDaniel ML (1986). A metabolite-regulated potassium channel in rat pancreatic B cells. *Proc Natl Acad Sci U S A* **83**, 7119–7123.

Nakazaki M, Ishihara H, Kakei M, Inukai K, Asano T, Miyazaki JI, Tanaka H, Kikuchi M, Yada T & Oka Y (1998). Repetitive mitochondrial Ca^{2+} signals synchronize with cytosolic Ca^{2+} oscillations in the pancreatic beta-cell line, MIN6. *Diabetologia* **41**, 279–286.

Nicholls DG & Ferguson SJ (2002). *Bioenergetics 3*. Academic Press, London.

Ortsater H, Liss P, Lund PE, Akerman KE & Bergsten P (2000). Oscillations in oxygen tension and insulin release of individual pancreatic ob/ob mouse islets. *Diabetologia* **43**, 1313–1318.

Panten U, Christians J, von Kriegstein E, Poser W & Hasselblatt A (1973). Effect of carbohydrates upon fluorescence of reduced pyridine nucleotides from perifused isolated pancreatic islets. *Diabetologia* **9**, 477–482.

Patterson GH, Knobel SM, Arkhammar P, Thastrup O & Piston DW (2000). Separation of the glucose-stimulated cytoplasmic and mitochondrial NAD(P)H responses in pancreatic islet beta cells. *Proc Natl Acad Sci U S A* **97**, 5203–5207.

Porksen N, Munn S, Steers J, Vore S, Veldhuis J & Butler P (1995). Pulsatile insulin secretion accounts for 70% of total insulin secretion during fasting. *Am J Physiol* **269**, E478–E488.

Porterfield DM, Corkey RF, Sanger RH, Tornheim K, Smith PJ & Corkey BE (2000). Oxygen consumption oscillates in single clonal pancreatic beta-cells (HIT). *Diabetes* **49**, 1511–1516.

Pralong WF, Bartley C & Wollheim CB (1990). Single islet beta-cell stimulation by nutrients: relationship between pyridine nucleotides, cytosolic Ca^{2+} and secretion. *EMBO J* **9**, 53–60.

Pralong W, Spat A & Wollheim C (1994). Dynamic pacing of cell metabolism by intracellular Ca^{2+} transients. *J Biol Chem* **269**, 27310–27314.

Robb-Gaspers LD, Burnett P, Rutter GA, Denton RM, Rizzuto R & Thomas AP (1998). Integrating cytosolic calcium signals into mitochondrial metabolic responses. *EMBO J* **17**, 4987–5000.

Rutter GA, Theler JM, Murgia M, Wollheim CB, Pozzan T & Rizzuto R (1993). Stimulated Ca^{2+} influx raises mitochondrial free Ca^{2+} to supramicromolar levels in a pancreatic beta-cell line. Possible role in glucose and agonist-induced insulin secretion. *J Biol Chem* **268**, 22385–22390.

Salvalaggio PR, Deng S, Ariyan CE, Millet I, Zawalich WS, Basadonna GP & Rothstein DM (2002). Islet filtration: a simple and rapid new purification procedure that avoids ficoll and improves islet mass and function. *Transplantation* **74**, 877–879.

Song SH, McIntyre SS, Shah H, Veldhuis JD, Hayes PC & Butler PC (2000). Direct measurement of pulsatile insulin secretion from the portal vein in human subjects. *J Clin Endocrinol Metab* **85**, 4491–4499.

Sturis J, Pugh WL, Tang J, Ostrega DM, Polonsky JS & Polonsky KS (1994). Alterations in pulsatile insulin secretion in the Zucker diabetic fatty rat. *Am J Physiol* **267**, E250–E259.

Tornheim K (1997). Are metabolic oscillations responsible for normal oscillatory insulin secretion? *Diabetes* **46**, 1375–1380.

Westerlund J & Bergsten P (2001). Glucose metabolism and pulsatile insulin release from isolated islets. *Diabetes* **50**, 1785–1790.

Worley JF III McIntyre MS, Spencer B, Mertz RJ, Roe MW & Dukes ID (1994). Endoplasmic reticulum calcium store regulates membrane potential in mouse islet beta-cells. *J Biol Chem* **269**, 14359–14362.

Yaney GC, Schultz V, Cunningham BA, Dunaway GA, Corkey BE & Tornheim K (1995). Phosphofructokinase isozymes in pancreatic islets and clonal beta-cells (INS-1). *Diabetes* **44**, 1285–1289.

Zhou YP, Pena JC, Roe MW, Mittal A, Levisetti M, Baldwin AC *et al*. (2000). Overexpression of Bcl-x_L in beta-cells prevents cell death but impairs mitochondrial signal for insulin secretion. *Am J Physiol Endocrinol Metab* **278**, E340–E351.

Acknowledgements

We wish to thank Dr James D. Johnson and Dr Wade L. Pearson for helpful discussions and Eric Ford for technical assistance and islet isolation. This work was supported by National Institutes of Health Grants DK31842 (to K.S.P) and DK37380 (to S.M.). D.S.L. received support from BioSim (EU Contract no. 005137) and Novo Nordisk A/S.